

**Gated Molecular Baskets**

Journal:	<i>Chemical Society Reviews</i>
Manuscript ID:	CS-REV-04-2014-000140.R1
Article Type:	Review Article
Date Submitted by the Author:	24-May-2014
Complete List of Authors:	Hadad, Christopher; The Ohio State University, Chemistry Hermann, Keith; The Ohio State University, Chemistry Ruan, Yian; The Ohio State University, Hardin, Alex; The Ohio State University, Chemistry; The Ohio State University, Badjic, Jovica; Ohio State University, Department of Chemistry

ARTICLE

Gated Molecular Baskets

Cite this: DOI: 10.1039/x0xx00000x

Keith Hermann, Yian Ruan, Alex M. Hardin, Christopher M. Hadad and Jovica D. Badjić*

Received 00th January 2012,
Accepted 00th January 2012

DOI: 10.1039/x0xx00000x

www.rsc.org/

In this review, we describe the construction of gated molecular baskets, discuss their mechanism of action in regulating the exchange of guests and illustrate the potential of these concave hosts to act as catalysts for controlling chemical reactions. Importantly, a number of computational and experimental studies have suggested that gated baskets ought to unfold their gates at the rim for permitting the passage of guests to/from their inner space. These dynamic hosts are therefore offered as useful models for investigating the process of gating in artificial systems. Furthermore, gated baskets should permit examining the benefit of controlling the rate by which reactants access a gated catalyst for promoting chemical reactions occurring in its confined space.

Introduction

Chemists have, for more than four decades, studied the characteristics and explored the utility of compounds with an enforced cavity.¹⁻³ At the present time, we recognize that cavitands would trap guest molecules that are complementary in shape, size and electronic attributes to their concave interior.⁴ In addition, the formation of such host-guest complexes is often driven by desolvation,^{5, 6} which plays an important role in complexation events.⁷ In his seminal paper about cavitand-based hosts,⁸ D. J. Cram discussed a prospective of using concave compounds for promoting chemical reactions,⁹⁻¹¹ stabilizing reactive intermediates¹²⁻¹⁵ and controlling the rates by which encapsulated molecules are undergoing in/out trafficking:¹⁶ "can cavitands be prepared with "pores" in their "skins" that allow the entrance and departure of certain guest from their interior, but forbid passage to others"? This intriguing question was of a great interest, soon thereafter the preparation of carcerands (Figure 1).^{17, 18} Namely, in 1985,

Several years later, soluble carcerand **2** was prepared¹⁸ and, with ¹H NMR spectroscopy, was shown to contain a molecule of templating solvent ((CH₃)₂SO, (CH₃)₂NCOCH₃, (CH₃)₂NCHO) in its cavity.^{17, 18} Indeed, when large C₅H₁₀NCHO solvent was used in the synthesis of **2** there was no formation of the host.^{18, 20} Interestingly, [2-(CH₃)₂SO] possessed a long lifetime with the entrapped DMSO molecule "unable" to depart from its inner space at 150°C for 24h!¹⁸ It was deduced that DMSO was permanently trapped in the cavity of **2** with its departure necessitating a cleavage of covalent bonds (>90 kcal/mol). The phenomenon is akin to mechanical bonds²¹ in rotaxanes for which a high activation barrier prevents the slippage of a macrocyclic ring over the bulky termini of its "axle-like" component.²²

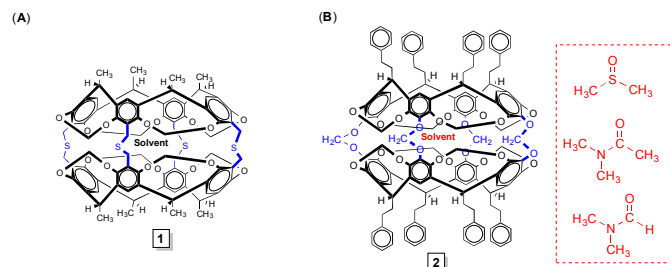


Figure 1. Chemical structures of carcerands **1** (A) and **2** (B). Three solvent molecules (red) were trapped in the cavity of **2** during its preparation.

the UCLA group reported the synthesis of *D*_{4h} symmetric host **1** (Figure 1A) with an enforced interior,¹⁹ although this molecular capsule was found to be poorly soluble in numerous solvents.

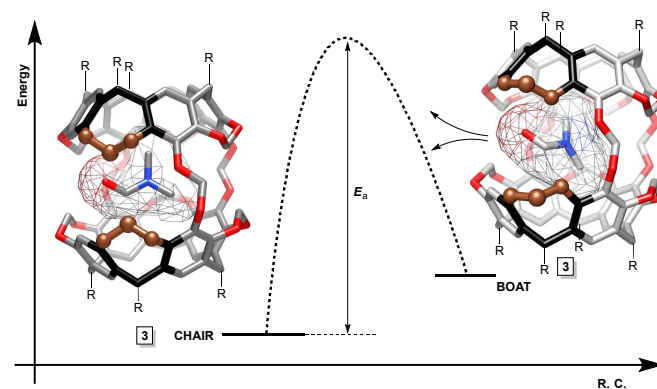


Figure 2. Dioxacyclooctadiene rings in hemicarcerand **3** (R = CH₂CH₂Ph) undergo chair-to-boat conformational changes. Two OCH₂O bridges (brown) alter the position to create a sizeable portal for a more facile trafficking of guests ((CH₃)₂NCHO is shown).

To reduce the high activation energy of the complexation/decomplexation of carcerands, Cram and co-workers designed hemicarcerands (Figure 2).²³ Molecular

capsule **3** ($R = \text{CH}_2\text{CH}_2\text{C}_6\text{H}_5$, Figure 2) was made²⁴ to carry three OCH_2O bridging units connecting its northern and southern cups. With one OCH_2O group missing, the side portal was, in hemicarcerand **3**, big enough to permit decomplexation ($E_a > 20$ kcal/mol) of several guests ($(\text{CH}_3)_2\text{SO}$, $(\text{CH}_3)_2\text{NCOCH}_3$, $(\text{CH}_3)_2\text{NCHO}$).^{25, 26} The activation energy of the process was indeed large, given a small affinity of guests for populating the host. Cram coined the term "constrictive binding"²⁷ to describe an apparent "physical barrier" corresponding to the guest departure. It derives from the Latin word *constrictus* meaning "narrowing of a passage". Questions about the nature of constrictive binding were posed, yet it was difficult addressing them with space-filling molecular models.²⁸ Houk and co-workers, however, were the first to show that conformational changes occurring within hemicarcerands ought to be considered for understanding the trafficking of molecules.²⁹ In particular, chair-to-boat interconversion of *one* dioxacyclooctadiene ring within carcerands/hemicarcerands was computed to require a considerable activation energy (>12 kcal/mol). The opening of *two* OCH_2O gates (>20 kcal/mol, Figure 2) was then proposed to promote access/departure of guests to/from the inner space of hemicarcerands (Figure 2).²⁸ If the host's dioxacyclooctadiene rings solely assume the chair conformation, the activation barrier for guest departure becomes insurmountable at experimentally accessible temperatures.³⁰ Almost two decades after the Houk's original proposal, the process of gating appears to be important for the operation^{31, 32} of various dynamic hosts.¹⁶ In addition, the gating could be used for developing supramolecular systems capable of controlling the outcome of chemical reactions^{33, 34} or delivery/trafficking of useful molecules.^{35, 36} In this review, we focus on describing the action of gated molecular baskets developed in our laboratory. These dynamic hosts are useful models for studying gated molecular encapsulation and its importance for controlling chemical reactivity.

A Case of Gated Encapsulation with the Formation of an Open-Host Intermediate

The entrapment of guests by gated hosts could, in some situations, be described with a mechanism (Figure 3) whereby the opening of the host (**H**) gives an unstable intermediate (**I**).³⁷

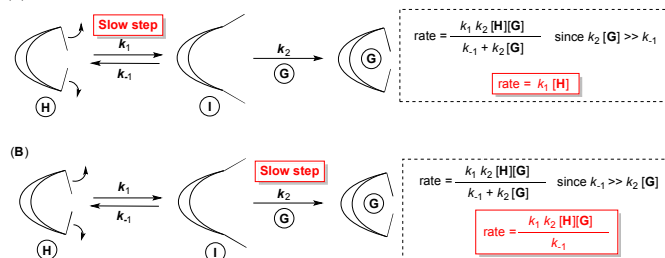


Figure 3. An exchange mechanism for gated encapsulation with the formation of intermediate **I**. The overall rate of the complexation could be a function of the concentration of guest **G** with two rate-limiting steps depending on its concentration: (A) step 1 with high $[\text{G}]$ and (B) step 2 with low $[\text{G}]$.

Accordingly, a conformational change in **H** could lead to **I** (Figure 3A/B), which then traps guest **G** in the step that follows. Accordingly, one can use the steady-state approximation to derive the corresponding rate law (Figure 3).³⁸ If the opening of host **H** is rate determining (step 1, Figure 3A), it follows that the encapsulation rate becomes solely a function of the concentration of host **H** ($\text{rate} = k_1 [\text{H}]$). Conversely, if the entrance of guest **G** into intermediate **I** is rate-determining (step 2, Figure 3B), then the rate becomes a function of the concentrations of both host **H** and guest **G** ($\text{rate} = k_{\text{obs}} [\text{H}] [\text{G}]$, Figure 3B). Rebek and co-workers used conventional kinetic analysis to examine the substitution of adamantane (**A**) inside "softball" host **4** with [2.2]paracyclophane (**P**) (Figure 4).³⁹ Self-assembled capsule **4** comprises a sizeable interior ($\sim 313 \text{ \AA}^3$) and is also made of two complementary subunits forming a seam of 16 hydrogen bonds (Figure 4).⁴⁰ Importantly, the affinity of **4** for entrapping

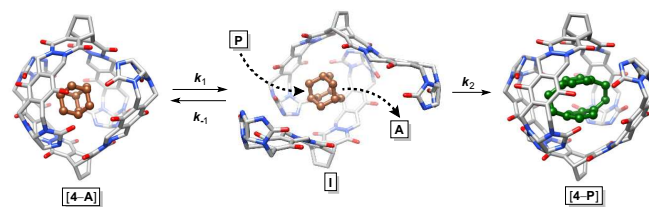


Figure 4. The proposed double-door gating mechanism for the conversion of softball-adamantane **[4-A]** complex into softball-paracyclophane **[4-P]**.

[2.2]paracyclophane is greater than for adamantane to permit practically irreversible conversion of **[4-A]** into **[4-P]** (Figure 4). The substitution was found to be slow enough and was monitored with conventional ^1H NMR spectroscopy using variable concentrations of compound **P**. At low concentrations of **P**, the reaction appeared to be first order in **P**, while at high concentrations of **P**, the complexation was zeroth order in this reactant! The saturation curve (k_{obs} vs $[\text{P}]$)³⁹ was taken as a sign for the formation of an intermediate and also a change in the rate-determining step of the substitution. The data were, subsequently, fit to the mechanistic scenario described in Figure 3 to give $k_1 = 0.0027 \text{ s}^{-1}$ ($\Delta G^\ddagger_1 = 20.3$ kcal/mol at 289 K). At high concentrations of **P**, the opening of capsule **4** is energetically demanding and limits the rate by which the supramolecular substitution takes place (Figure 3A). To examine the nature of the experimentally observed intermediate, Houk and co-workers computed⁴¹ that the formation of double-door **I** (Figure 4) would require ~ 24 kcal/mol, which is close to the experimentally observed ΔG^\ddagger_1 (20.3 kcal/mol).

In line with the discussion, the opening of hemicarcerands of type **3** (Figure 2) was computed³⁰ to constitute the rate-limiting step in the formation of hemicarceplexes.¹⁶ Additional experimental measurements,^{42, 43} however, remain to be completed to test such computational predictions.⁴⁴ Finally, the operation of gated molecular baskets (see below) constitute another mechanistic alternative with, perhaps, one elementary step including: the ingress of a guest, from bulk solvent, causing the egress of the residing guest and opening of the

basket's gates. The mechanism of action of gated molecular baskets is described in sections that follow.

Gated Molecular Baskets

Design and Preparation: We originally designed molecular baskets of type **5** (Figure 5, R = CH₃) in our laboratory.⁴⁵ The key reaction for the preparation of these dynamic hosts is the *tris*-annulation of racemic norbornene compounds using transition metal catalyst(s), either Cu(I) or Pd(0) (Figure 5A).^{46, 47} In particular, De Lucchi and co-workers have developed⁴⁸ a variety of useful cyclotrimerization protocols. The reaction gives a mixture of *syn/anti* diastereomeric products (Figure 5A) for which the undesired *anti* compound usually dominates. To overcome this difficulty, we optimized a methodology for

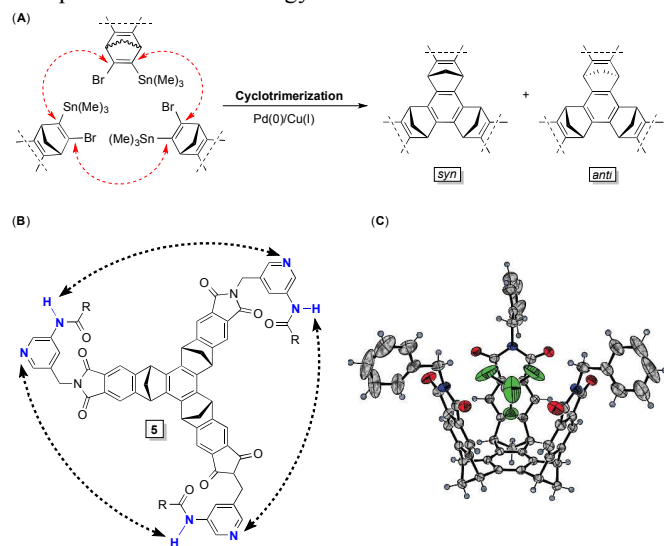


Figure 5. (A) The *tris*-annulation of stannylated norbornenes is promoted with Cu(I) or Pd(I) catalysts to give a mixture of *syn* and *anti* cyclotrimers. (B) Chemical structure of gated molecular baskets (**5**, R = CH₃) with three intramolecular N–H...N hydrogen bonds. (C) ORTEP representation of the solid-state structure of a gated basket,⁴⁵ note that a molecule of CHCl₃ resides in the cavity of this host having three phenyl gates at the rim.

enantiodiscrimination of racemic norbornene reactants using metal cations (Cu(I)/Cs(I)) as templates to favour the formation of the *syn* product.⁴⁶ Molecular baskets of type **5** (Figure 5B/C) are C₃ symmetric compounds with a flat aromatic base fused to three bicyclo[2.2.1]heptane rings to form a curved unit. Three phthalimides extend this semi-rigid structure into a bowl-shaped cavitand (Figure 5C). The pyridine-based gates are each conjugated to the framework via a CH₂ rotor and are also equipped with an amide functional group.⁴⁹ The amide units are predisposed to, in non-competitive organic solvents,⁵⁰ form a seam of N–H...N intramolecular hydrogen bonds (Figure 5B) and thereby enclose space to give rise to a molecular capsule (Figure 6). In principle, multivalent **5** could also undergo *intermolecular* aggregation, and we used vapour pressure osmometry (VPO), mass spectrometry, FT-IR and DOSY ¹H-NMR spectroscopic methods^{45, 49} to show that **5** stays monomeric in nonpolar organic solvents (CDCl₃, CD₂Cl₂, etc.).

Furthermore, the amide groups were found to adopt a Z configuration about each C–N bond with the basket's pyridine gates forming three *intramolecular* N–H...N hydrogen bonds (Figure 5B);⁴⁹ ¹H NMR chemical shifts of the singlet corresponding to the N–H protons are typically found at δ > 11 ppm.

Encapsulation Thermodynamics: To evaluate the internal volume of energy-optimized **5** (DFT, B3LYP/6–31G(d)),⁴⁷

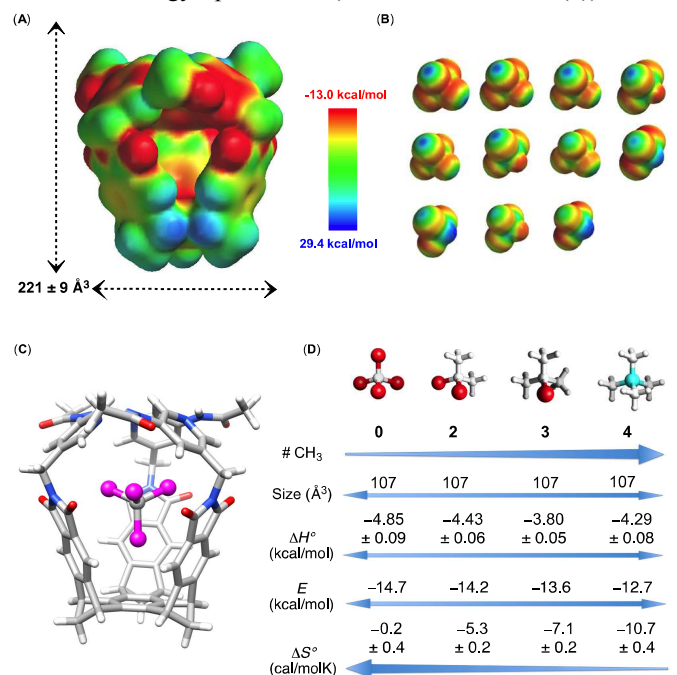


Figure 6. EPS surfaces (AM1, Spartan) of gated molecular basket **5** (V = 226 Å³, A) and small haloalkanes (V = 80–110 Å³, B). (C) Energy-minimized (DFT, M05-2X/6-31+G(d,p)) structure of complex [**5**–CBr₄] showing the most favourable orientation of CBr₄ guest inside this gated host. (D) Thermodynamic data corresponding to the complexation of CBr₄, CBr₂(CH₃)₂, CBr(CH₃)₃ and Si(CH₃)₄ with basket **5** in CH₂Cl₂.

with its pyridine gates in their "closed" position (226 Å³, Figure 6A), we used the 3V software.⁵¹ While this particular freeware was originally recommended for investigating drug-binding sites in biological molecules,⁵² it can also be used for studying artificial hosts.⁵¹ The computed electrostatic potential surface (AM1, Spartan) of the interior of C₃ symmetric **5** encompasses domains with negative potentials⁵³ making it complementary to tetrahedral haloalkanes (V = 80 – 110 Å³, Figure 6B). In fact, haloalkane guests are poised⁴⁷ to place one of their polarizable groups against the cup-shaped framework of **5** with the remaining three units pointing to side portals (Figure 6C). With the assistance of variable temperature ¹H NMR spectroscopy,^{47, 49} we demonstrated that a small haloalkane (CCl₄, CBr₄, CH₃CBr₃, etc.) would occupy the inner space of **5** in solvophobic CH₂Cl₂ (61 Å³).⁵¹ Notably, the binding energy was found to be a function of the guest's size with ΔG° = –4.85 ± 0.1 kcal/mol (298.0 K) for bigger CBr₄ (106 Å³) and ΔG° = –1.0 ± 0.1 kcal/mol (298.0 K) for smaller CHBr₃.⁵⁴ The affinity tracked the population of the inner space of gated **5** (expressed via so-called packing coefficient, PC = V_{guest}/V_{host})⁵⁵ whereby the PC of CBr₄ is 0.47 while for CHBr₃ is 0.39. Interestingly,

all encapsulations were driven by enthalpy ($\Delta H^\circ < 0$) due to, perhaps, the complementarity of host and guests in shape and electrostatic characteristics (Figure 6A/B). We further examined the binding of four guests with similar volumes having a variable number of CH₃ groups (Figure 6D).⁴⁷ The enthalpy of the interaction was comparable along the series ($\Delta H^\circ \sim -4$ kcal/mol), and in line with the computed energies (E , Figure 6D). The entropic contribution, however, changed: the greater the number of CH₃ groups, the more negative ΔS° (from -0.2 to -10.7 e.u., Figure 6D). Presumably, the motion of methyl groups becomes restricted in the cavity of gated basket **5** to contribute to the effect. There is roughly ~ 0.6 – 1 kcal/mol loss in energy ($T\Delta S^\circ$) per each additional CH₃ group at 298 K.

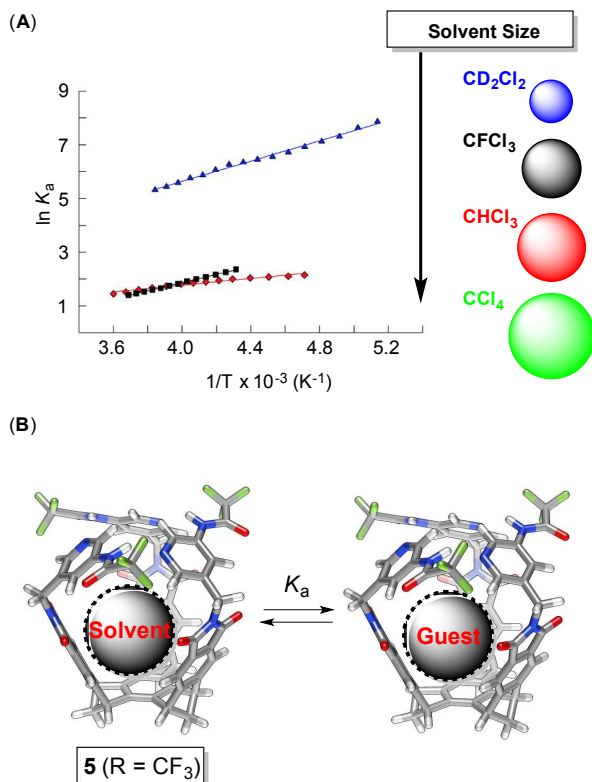


Figure 7. (A) The affinity of (CH₃)₂CBr₂ ($\ln K_a$) for occupying the cavity of **5** and giving [5–(CH₃)₂CBr₂] was measured (¹H NMR spectroscopy) in four differently sized solvents (colour coded) at various temperatures; In CCl₄ (green), the complexation was too weak to quantify by ¹H NMR spectroscopy. (B) In solution, basket **5** is occupied by guest or solvent molecules, and the equilibrium (K_a) for guest association is a function of the relative stability of the two complexes.

Finally, we quantified the potential of **5** (R = CF₃, Figure 7) for trapping 2,2-dibromopropane (107 Å³, $PC = 0.47$) in four differently sized solvents having comparable polarities: CD₂Cl₂ (61 Å³), CDCl₃ (75 Å³), CFC₃ (81 Å³) and CCl₄ (89 Å³).⁵¹ The stability of [5–(CH₃)₂CBr₂] was found to be higher in CD₂Cl₂ while lower in CDCl₃/CFC₃ and very small in CCl₄ (Figure 7A).⁵¹ Apparently, the smallest dichloromethane is the least competitive solvent in the series with the lowest affinity for occupying the basket (Figure 7B)!⁷ We reasoned that in line with the encapsulation stoichiometry (Figure 7B),^{51, 56} one CD₂Cl₂ is too small ($PC = 0.28$), while two are incompatible in shape with the interior of **5** to populate it. When more sizeable

solvents (C₆D₆ (99 Å³), C₆D₅CD₃ (117 Å³), *m*-C₆D₃(CD₃)₂ (136 Å³) and 1,3,5-C₆D₃(CD₃)₃ (154 Å³) were probed as a medium for the encapsulation of haloalkanes,⁵⁷ the solubility of "free" basket **5** dropped, albeit it improved considerably in the presence of guests (i.e. [5–guest] complexes). Importantly, the affinity of **5** for trapping 1,1,1-tribromoethane increased in the series with mesitylene being the most solvophobic medium ($K_a = 4123 \text{ M}^{-1}$, 300.0 K). The finding bodes well with the encapsulation stoichiometry (Figure 7B) in which a trapped guest molecule is substituted with the solvent: [5–mesitylene] complex possesses the lowest stability ($PC = 0.68$) to contribute to a greater quantity of [5–guest]. Furthermore, the finding is in line with the W. C. Still's pioneering study⁷ on elucidating the importance of solvent size for the formation of encapsulation complexes.

Stimuli-Responsive Behaviour: The preparation and study of switchable hosts could be of interest for developing more sophisticated catalysts,^{58–60} energy conversion devices^{61–63} and sensors.⁶⁴ Despite much advancement in the field,^{65–69} attaining control over conformational dynamics and functional behaviour of molecules, or their assemblies, remains a challenge.^{70–73} Accordingly, we studied⁷⁴ switchable characteristics of gated

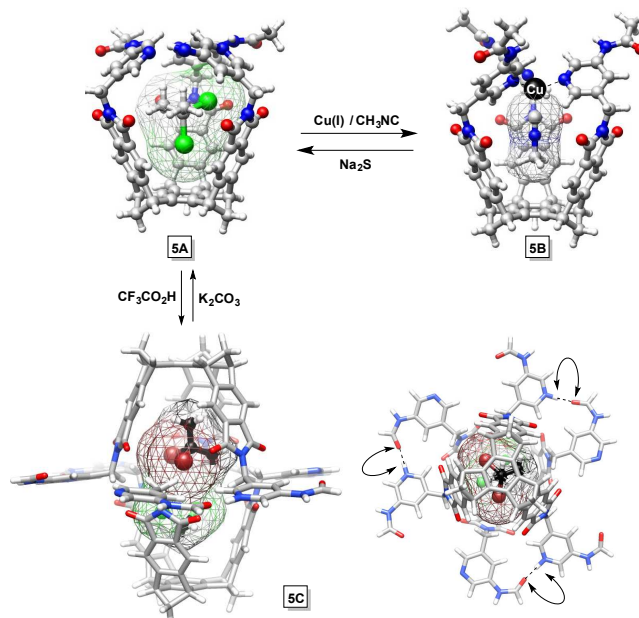


Figure 8. Energy-minimized structures (MMFFs, Spartan) of baskets [5A–((CH₃)₂CBr₂)], [5B–(CH₃NC)] and [5C–((CH₃)₂CBr₂)/CH₂Cl₂]; note that side and top views of [5C–((CH₃)₂CBr₂)/CH₂Cl₂] are shown.

molecular baskets and found that these hosts can be reversibly interconverted among conformational states **5A**, **5B** and **5C** (Figure 8). Importantly, each state has unique encapsulation characteristics and distinct internal dynamics. Gated basket **5A** (226 Å³) contains three pyridine-based gates for forming a seam of intramolecular N–H...N hydrogen bonds and occluding space. This host was found (¹H NMR spectroscopy) to selectively trap 2,2-dibromopropane ((CH₃)₂CBr₂, 107 Å³) in the presence of methylisocyanide (CH₃NC, 58 Å³).⁷⁴ Upon addition of an equimolar amount of (CuOTf)₂PhMe, however,

we observed (^1H NMR spectroscopy) the conversion of basket **5A** into **5B** (Figure 8). Importantly, **5B** contains Cu(I) cation at its rim coordinating to sp^2 nitrogen atoms of the pyridine gates and also a molecule of CH_3NC occupying the host's cavity.⁷⁵⁻⁷⁷ The use of external chemical stimulus (Cu(I)) therefore caused a disruption of three N–H---N hydrogen bonds in **5A**, reorganization of its gates and finally exchange of guests to give rise to **5B**. To reverse these chemical changes, we used Na_2S which coordinated to Cu(I) and thereby triggered the conversion of **5B** back into **5A**. Following, we added trifluoroacetic acid (TFA, $\text{p}K_{\text{a}} = -0.25$) to **5A** to induce the protonation of pyridine gates ($\text{p}K_{\text{a}} = 5.25$). Indeed, the protonation took place, and we observed the dimerization of the host to give **5C** (Figure 8): the assembly comprised three $^+\text{N-H---O}$ hydrogen bonds between the pyridine gates of the baskets at the southern and northern termini of such dimeric structure (Figure 8). Self-assembled **5C** has a spacious interior (307 \AA^3) that allowed simultaneous trapping of $(\text{CH}_3)_2\text{CBr}_2$ and CD_2Cl_2 in its cavity.⁷⁴ Finally, the addition of K_2CO_3 to **5C** led to its full deprotonation and the formation of **5A** for completing the acid-base cycle (Figure 8).

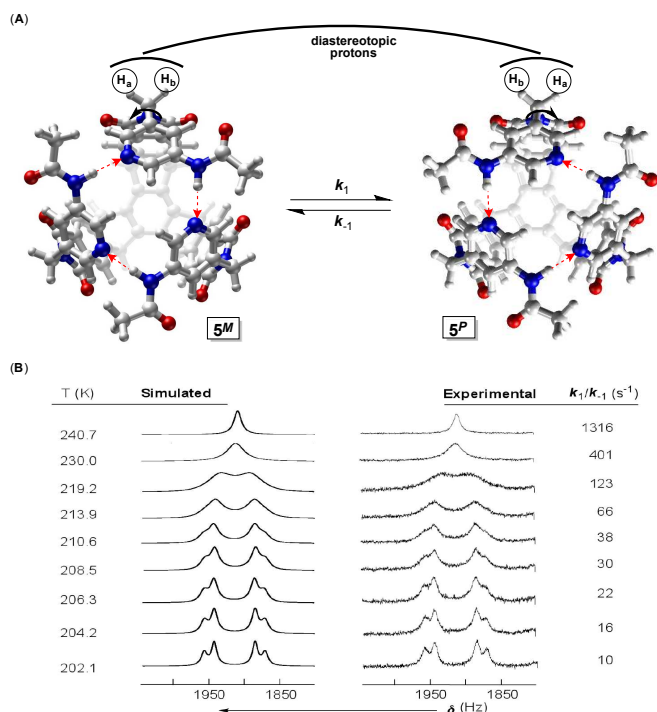


Figure 9. (A) Top views of stereoisomeric baskets **5^M** and **5^P** (MMFFs, Spartan). (B) A segment of simulated (WinDNMR) and experimental VT ^1H NMR spectra of basket **5** ($\text{R} = \text{CH}_3$) in CD_2Cl_2 , showing the coalescence of the AB quartet, corresponding to CH_2 protons, into a singlet.⁴⁹

Conformational Stereoisomerism and Racemization: In **5**, the seam of N–H---N hydrogen bonds can be oriented in two directions (*P* or *M*) to give stereoisomeric baskets **5^P** and **5^M** (Figure 9A).⁴⁹ Thus, in solution, the rotation of the pyridine gates, assuming propeller-like orientations, should permit the interconversion of dynamic enantiomers **5^P** and **5^M**. In line with this reasoning, ^1H NMR signals corresponding to CH_2 hydrogen

nuclei in **5** are expected to become diastereotopic during a slow racemization (Figure 9A). When the exchange of CH_2 signals is, however, fast on the NMR time scale, these protons become enantiotopic and therefore indistinguishable by dynamic ^1H NMR spectroscopy. Indeed, variable temperature ^1H NMR spectroscopy (VT ^1H -NMR) corroborated the anticipated scenario for the racemization of **5^{P/M}**: the resonance corresponding to CH_2 group appeared as a singlet at high but AB quartet at low temperatures (Figure 9B).⁴⁹ The data were subjected to total band-shape analyses to obtain first-order rate coefficients k_1/k_{-1} corresponding to the basket's opening and closing ($\Delta G_{\text{rac}}^\ddagger \sim 9\text{--}13 \text{ kcal/mol}$, Figure 9B).^{78, 79} Interestingly, the rate of racemization appeared to be a function of the guest's affinity for occupying the basket's cavity: the greater the affinity (ΔG°), the slower the **5^{P/M}** interconversion ($\Delta G_{\text{rac}}^\ddagger$)!⁷⁹ To account for the observation, we reason that a greater host-guest affinity means a stronger intermolecular attraction and thereby a greater "pull" on the gates by the guest to decrease the rate by which the basket opens and closes its gates; note that the situation is somewhat complicated by the fact that guest exchange could also contribute to the revolving of three aromatic gates (see below).⁵⁶ To further investigate the mechanism of **5^{P/M}** interconversion, we used VT ^1H -NMR spectroscopy to quantify the racemization of **5** ($\text{R} = \text{CF}_3$, Figure 5) in four differently sized solvents (CD_2Cl_2 (61 \AA^3), CDCl_3 (75 \AA^3), CFCl_3 (81 \AA^3) and CCl_4 (89 \AA^3)).⁵¹ Interestingly, the racemization was found to be fastest in CD_2Cl_2 ($\Delta G_{\text{rac}}^\ddagger = 10.9 \pm 0.3 \text{ kcal/mol}$ at 298.0 K) while slowest in CCl_4 ($\Delta G_{\text{rac}}^\ddagger = 12.8 \pm 0.2 \text{ kcal/mol}$ at 298.0 K). When $\Delta H_{\text{rac}}^\ddagger$ was plotted against

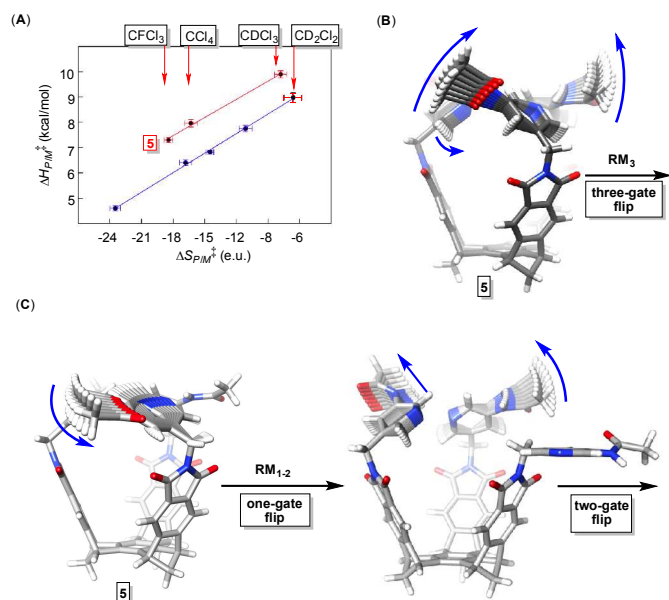


Figure 10. The enthalpy/entropy compensation relationships corresponding to the racemization of gated basket **5** (red, $R^2 = 0.999$) and another more spacious gated basket ($V = 318 \text{ \AA}^3$, blue) in four differently sized solvents. (B) Three-gate racemization mechanism (RM_3) was computed (B3LYP/6-31+G(d,p)//PM6) to proceed via simultaneous rotation of all three gates. (C) One/two gate racemization mechanism ($\text{RM}_{1,2}$) was computed (B3LYP/6-31+G(d,p)//PM6) to proceed via rotation of one gate followed by simultaneous rotation of the remaining two gates.

$\Delta S_{\text{rac}}^{\ddagger}$ (red line in Figure 10A), however, we found an isokinetic relationship for the interconversion of $5^{P/M}$ in CDCl_3 , CFCl_3 and CCl_4 suggesting the same mechanism of racemization.⁵¹ The interconversion of $5^{P/M}$ in CD_2Cl_2 was, however, found to fit to another isokinetic relationship (blue line in Figure 10A) suggesting a different racemization pathway;⁵¹ note that this particular linear dependence corresponded to the racemization of a more spacious gated basket in the same four solvents. Markedly, the population of the basket's cavity varies for the examined solvents, acting as guests: while the PC for CDCl_3 , CCl_4 and CFCl_3 varies from 0.33 to 0.39, it is 0.27 for CD_2Cl_2 . In line with the experimental evidence (Figure 10A), we went on to suggest that the size of guests residing inside gated baskets of type **5** matter in the opening/closing event by imposing on the operation of gates revolving at the rim. That is to say, when $PC > 0.30$, the racemization of basket follows the mechanistic pathway whereby all three gates revolve simultaneously (RM_3 , Figure 10B). However, for $PC < 0.30$, the revolving mechanism comprises one pyridine gate "breaking away" from the $\text{N-H}\cdots\text{N}$ hydrogen bonding to form an intermediate state followed by the concomitant flip of the remaining two gates (RM_1 , Figure 10). The reasoning is in line with our computational study whereby the RM_3 pathway dominates for the racemization of baskets having pyridine gates forming stronger intramolecular $\text{N-H}\cdots\text{N}$ hydrogen bonding contacts.⁵¹

Encapsulation Kinetics: To examine the rate law characterizing the exchange of 1,1,1-trichloroethane (CH_3CCl_3) to/from gated basket **5** ($R = \text{Ph}$, Figure 5), we completed ^1H , ^1H -

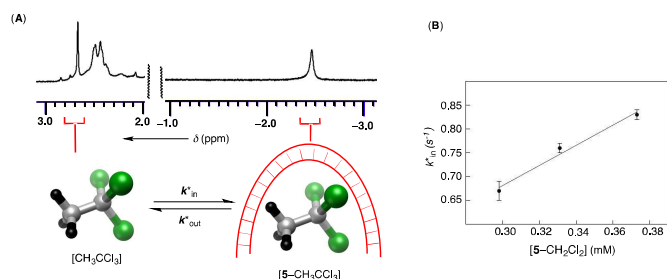


Figure 11. (A) ^1H NMR signals corresponding to hydrogen nuclei of CH_3CCl_3 residing in bulk CD_2Cl_2 solvent ($\delta = 2.70$ ppm) and inside basket **5** ($\delta = -2.45$ ppm) recorded at 250 K. (B) A plot showing magnetization rate constants k_{in}^* (^1H , ^1H - EXSY, 250.0 K) as a linear function of the concentration of free basket $[5-\text{CH}_2\text{Cl}_2]$ in solution.

EXSY and selective inversion-transfer NMR measurements.⁵⁶ These experiments were conducted under equilibrium conditions, with the exchange rate constants k_{in}^* (s^{-1}) and k_{out}^* (s^{-1}) characterizing the transfer of longitudinal magnetization of CH_3CCl_3 nuclei from bulk solvent to the interior of gated basket and vice versa (Figure 11A).^{80, 81} On the basis of already established 1:1 host/guest binding stoichiometry (*vide supra*),⁴⁷ we assumed that the formation of $[5-\text{CH}_3\text{CCl}_3]$ is first order in $[5-\text{CH}_2\text{Cl}_2]$ and $[\text{CH}_3\text{CCl}_3]$ so that $v_{\text{in}} = k_{\text{in}} [5-\text{CH}_2\text{Cl}_2] [\text{CH}_3\text{CCl}_3]$; note that CD_2Cl_2 is bulk solvent, occupying "free" basket **5**. Since the rate of the forward reaction, from the magnetization transfer experiments, is formulated as $v_{\text{in}} = k_{\text{in}}^*$

$[\text{CH}_3\text{CCl}_3]$,⁸⁰ we arrived to the following dependence: $k_{\text{in}}^* = k_{\text{in}} [5-\text{CH}_2\text{Cl}_2]$. If the proposed kinetic model is valid, the experimentally determined k_{in}^* must be a linear function of the concentration of basket $[5-\text{CH}_2\text{Cl}_2]$. Indeed, we found a linear dependence between k_{in}^* and $[\text{CH}_3\text{CCl}_3]$ with the slope of the fitted curve equal to $k_{\text{in}} = 2.1 \pm 0.3 \times 10^3 \text{ M}^{-1}\text{s}^{-1}$ ($\Delta G_{\text{in}}^{\ddagger} = 10.7$ kcal/mol, Figure 11B).^{56, 79} Following, the rate law corresponding to CH_3CCl_3 guest departing $[5-\text{CH}_3\text{CCl}_3]$ complex was, in a similar manner,⁵⁶ probed by varying the concentration of $[\text{CH}_3\text{CCl}_3]$ and measuring k_{out}^* (^1H NMR spectroscopy). Importantly, there was no interdependence between the experimentally determined k_{out}^* and $[\text{CH}_3\text{CCl}_3]$ to suggest that the departure of this guest from $[5-\text{CH}_3\text{CCl}_3]$ is zeroth order in its concentration with the rate law $v_{\text{out}} = k_{\text{out}} [5-\text{CH}_3\text{CCl}_3]$ ($k_{\text{out}}^* = k_{\text{out}} = 10 \text{ s}^{-1}$; $\Delta G_{\text{out}}^{\ddagger} = 13.4$ kcal/mol). At last, the activation energy for the racemization of $[5-\text{CH}_3\text{CCl}_3]$ was (from dynamic ^1H NMR spectroscopy)⁴⁹ determined to be $\Delta G_{\text{rac}}^{\ddagger} = 11.7$ kcal/mol; the racemization of $[5-\text{CH}_2\text{Cl}_2]$ was, however, more facile with $\Delta G_{\text{rac}}^{\ddagger} = 9.2$ kcal/mol.

The Mechanism of Gated Encapsulation: The results of steered molecular dynamics calculations showed that "opening" of three pyridine-based gates is required for the trafficking of guests to/from baskets (Figure 12A).⁷⁹ In particular, pulling CH_3CCl_3 from the interior of $[5-\text{CH}_3\text{CCl}_3]$, along various reaction trajectories, would cause a rupture of $\text{N-H}\cdots\text{N}$ hydrogen bonds.⁵⁶ Ergo, the unfolding of pyridine gates within gated baskets must occur with the departure of guests. As discussed in the previous section, the rate law corresponding to

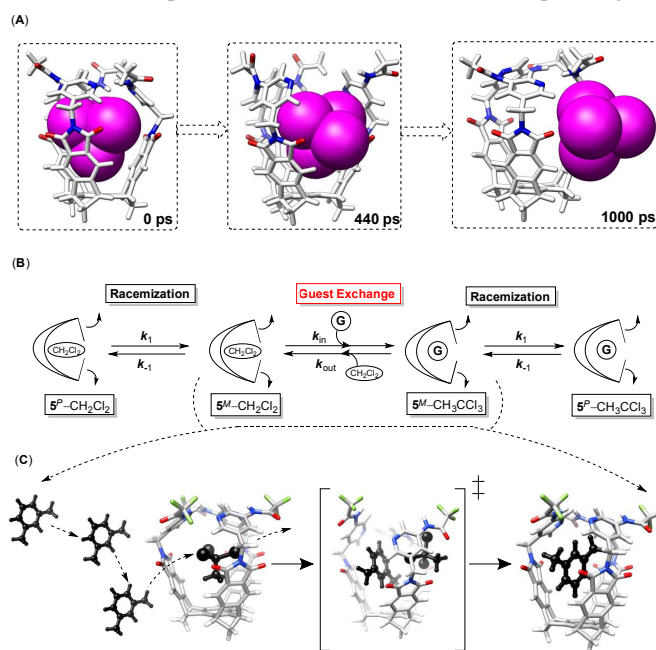


Figure 12. (A) Snapshots of guest CBr_4 departing basket **5** ($R = \text{Ph}$), along a force vector aligned with the basket's side aperture, obtained from steered molecular dynamics simulations.⁷⁹ (B) The proposed mechanism of guest/solvent exchange for gated baskets of type **5**. (C) A supramolecular substitution reaction with a molecule of solvent (*m*-xylene) displacing CH_3CBr_3 residing in the cavity of gated basket **5**.

the formation of $[5-CH_3CCl_3]$ complex ($v_{in} = k_{in}$ $[5-CH_2Cl_2][CH_3CCl_3]$) was found to be first-order in guest suggesting that ingress/egress of CH_3CCl_3 constitutes the rate-limiting step of gated encapsulation (Figure 12B). Finally, the racemization of $[5-CH_3CCl_3]$ ($\Delta G_{rac}^{\ddagger} = 11.7$ kcal/mol) was found to be more facile than the departure of CH_3CCl_3 from $[5-CH_3CCl_3]$ complex ($\Delta G_{out}^{\ddagger} = 13.4$ kcal/mol). Apparently, gated host $[5-CH_3CCl_3]$ incessantly flutters its pyridine gates at the rim ($\Delta G_{rac}^{\ddagger} = 11.7$ kcal/mol). An occasional egress of CH_3CCl_3 and ingress of CD_2Cl_2 ($\Delta G_{out}^{\ddagger} = 13.4$ kcal/mol) takes place to give $[5-CH_2Cl_2]$. The presumption is that CD_2Cl_2 enters gated basket of type **5** via a sizeable side aperture to substitute CH_3CCl_3 in a single elementary step (Figure 12C);⁵⁷ indeed, there could be an intermediate (i.e. partly-unfolded basket) forming along the way.³⁹ More experiments are needed to refute/confirm such a mechanistic scenario. Lastly, we discovered that the rate of the solvent/guest supramolecular substitution (Figure 12C) is, in gated encapsulations, a function of the size of solvent molecules displacing the entrapped guest: the bigger the solvent the slower the displacement.⁵⁷ The negative entropy of activation ($\Delta S^{\ddagger} < 0$) is, furthermore, characterizing such transformations with a transition state (Figure 12C) comprising both guest and solvent molecules within the gated host.⁵⁷

Controlling the Encapsulation Kinetics: There has been some interest toward understanding the persistency (lifetime) of encapsulation complexes.⁸²⁻⁸⁶ Indeed, a control of the host's dynamics⁸⁷ could be useful for regulating the outcome of chemical reactions⁸⁸ and delivering compounds at a precise

should allow the preparation of novel supramolecular catalysts (*vide infra*).⁹³⁻⁹⁵ Gated baskets of type **5** operate by unfolding pyridine-based gates at the rim for permitting in/out exchange of guests. It follows that adjusting the rate (k_{rac}) by which gates revolve ought to affect the residing time ($t = 1/k_{out}$) of trapped compounds.⁹⁶ In accord with this reasoning, we decided to alter the electronic and steric characteristics of R amido groups in basket **5^R** (Figure 13A), with the notion that these substituents would, to a variable degree, affect the stability of the N-H...N hydrogen bonds.⁹⁷ By altering the racemization rate of **5^R**, we should change the kinetic lability of noncovalent complexes. Since weak/moderate hydrogen bonds are electrostatic in nature, the electron-density perturbations of **5^R** had to be anisotropic to affect the host's dynamics in the desired manner: a depletion of the charge at N-H⁺ positions should be accompanied by a negligible perturbation at the Pyr-N: sites. Indeed, computed electrostatic potentials (HF(6-31G(d,p))⁹⁶ suggested a fluctuation in the charge density at the hydrogen atom of N-H groups, but rather consistent values at the pyridine nitrogen atoms.

With the assistance of ¹H NMR spectroscopy (¹H, ¹H-EXSY) we found that electron-withdrawing CF₃ groups in **5^{CF3}** (Table 1) retarded, while electron-donating CH₃ groups in **5^{CH3}** accelerated, the racemization of these baskets. More importantly, the rate coefficient (k_{out} , Table 1) characterizing

Table 1. Kinetic parameters for the racemization (k_{rac} , ¹H NMR line-shape analysis) of $[5^R-(CH_3)_3CBr]$ and the departure of *t*-BuBr (k_{out} , 2D ESXY NMR) from $[5^R-(CH_3)_3CBr]$, at 226.0 K. Thermodynamic stabilities (ΔG° , 226.0 K) of $[5^R-(CH_3)_3CBr]$ encapsulation complexes.⁹⁶

Basket 5^R	k_{rac} (s ⁻¹)	k_{out} (s ⁻¹)	ΔG° (kcal/mol)
CH ₃	108 ± 22	4.7 ± 0.7	-2.1 ± 0.1
(CH ₃) ₃ C	78 ± 16	11.5 ± 0.9	-2.3 ± 0.1
CH ₃ (CH ₂) ₅	97 ± 20	4.3 ± 0.4	-2.0 ± 0.1
CH ₃ CH=CH	83 ± 17	2.8 ± 0.1	-2.0 ± 0.1
C ₆ H ₅	20 ± 4	0.4 ± 0.1	-2.0 ± 0.2
CF ₃	4 ± 1	0.07 ± 0.02	-1.0 ± 0.2

the departure of $(CH_3)_3CBr$ guest from $[5^R-(CH_3)_3CBr]$ followed the same trend! The kinetic stability of $[5^R-(CH_3)_3CBr]$ decreased in the series in spite of a comparable thermodynamic stability of these complexes ($\Delta G^\circ \sim -2$ kcal/mol, Table 1). In fact, the thermodynamically least stable complex $[5^{CF_3}-(CH_3)_3CBr]$ ($\Delta G^\circ = -1.0 \pm 0.2$ kcal/mol, Table 1) was also the most persistent one ($k_{out} = 0.07 \pm 0.02$ s⁻¹). The lifetime ($t = 1/k_{out}$, Figure 13A) of encapsulation complexes $[5^R-(CH_3)_3CBr]$ is thus a function of the dynamics of the pyridine-based gates: the more sluggish the gates, the more persistent the encapsulation complex. Lastly, the kinetic data for the departure of $(CH_3)_3CBr$ was placed on a quantitative scale using Taft's linear free-energy relationship (Figure 13B).⁹⁸ The Taft's scale defines polar (σ^*) and steric (E_s) constants of a variety of substituents and has been useful for studying the perturbation of both equilibria and rates of chemical reactions.⁹⁹ We used this two-parameter model to fit a linear dependence between $\log(k_{out}^{(R)}/k_{out}^{(Me)})$ and $\rho^* \sigma^* + \delta E_s$ (Figure 13B). The correlation was acceptable ($R^2 = 0.94$), with the departure rates being a function of both electronic ($\rho^* = -0.6$) and steric

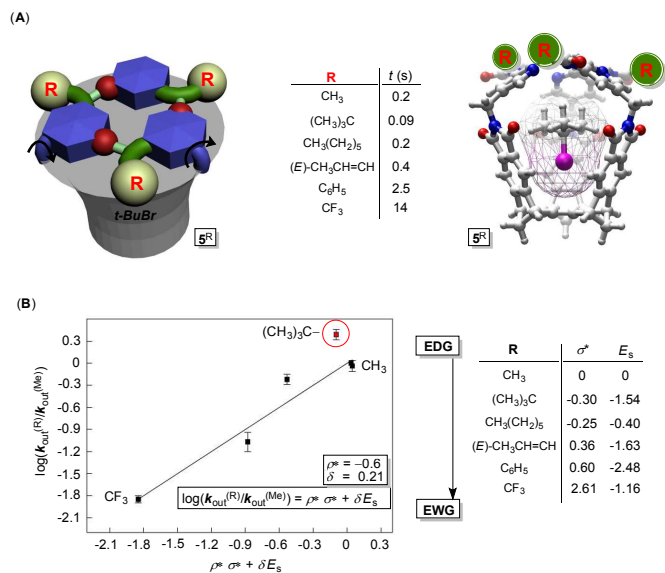


Figure 13. (A) Schematic (left) and energy-minimized (right) representations of gated molecular baskets **5^R** capable of controlling time ($t = 1/k_{out}$) that *t*-BuBr spends in their cavity. (B) Linear free-energy relationship corresponding to the dissociation of *t*-BuBr from baskets **5^R**. The correlation ($R^2 = 0.94$) was obtained using Taft's two-parameter regression model with polar (σ^*) and steric (E_s) substituent constants.

rate.^{89, 90} In line with studying molecular gating, we realized that learning about conformational changes in cavitand-based hosts^{91, 92} and understanding how to fine-tune such processes

($\delta = 0.2$) characteristic of the amido substituents. Evidently, one can predict and fine-tune the residing time of guests within a cavity of gated hosts!

On the Shape Selectivity: If two guests possess the same affinity for occupying a gated basket (ΔG°), will they enter such host at the same rate ΔG_{in}^\ddagger ? How do size, shape and/or

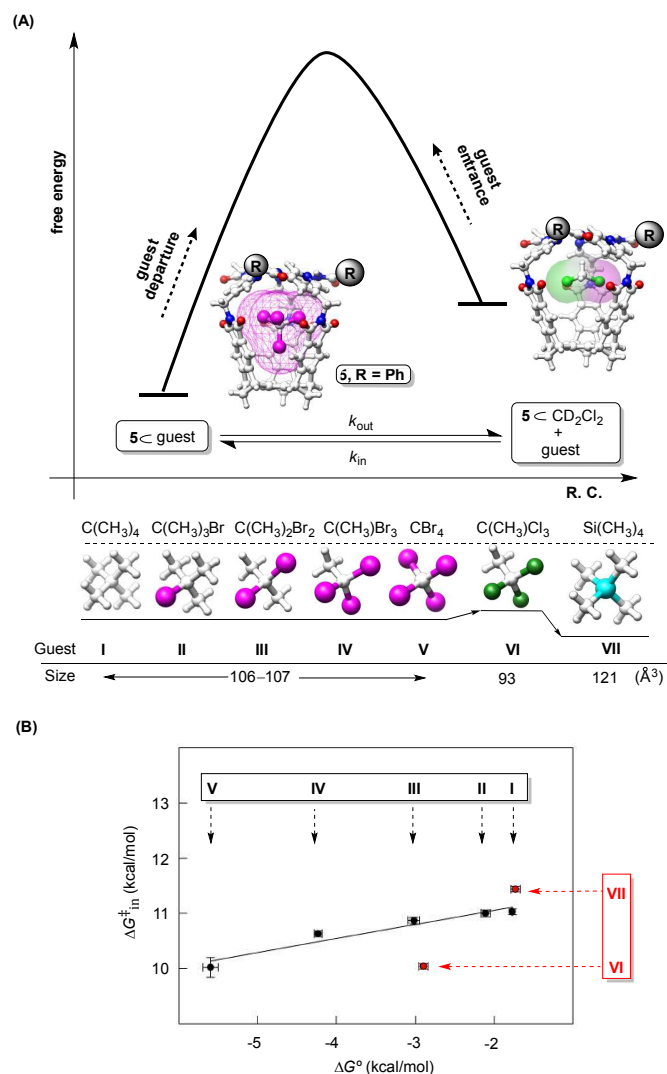


Figure 14. (A) (Top) Reaction coordinate diagram showing an equilibrium with guests I–V (CBr₄ is displayed) entering (k_{in}) and departing (k_{out}) gated molecular basket 5 (R = Ph). Solvent molecule CD₂Cl₂ occupies basket 5 devoid of external guests. (Bottom) Energy-minimized structures (DFT, B3LYP/3-21G) of guests I–VII and their corresponding volumes (Å³). (B) Activation energies for guests I–V (black) entering (ΔG_{in}^\ddagger) basket 5 were found to be a linear function of the corresponding binding energies (ΔG° , 250.0 ± 0.1 K). The kinetic behaviour of smaller VI (93 Å³) and bigger VII (121 Å³) guests deviates from the observed linear free-energy relationship ($\Delta G_{in}^\ddagger = \rho \Delta G^\circ + \delta$).

thermodynamic affinity (ΔG°) affect the encapsulation kinetics? Can we derive rules to describe how gated baskets of type 5 (Figure 14) differentiate among guest molecules? To address these intriguing questions, we chose to study the kinetics and thermodynamics of the encapsulation of I–V (Figure 14A) with basket 5 (R = Ph, Figure 14A) in CD₂Cl₂.^{78, 79} Compounds I–V are isosteric (V = 106–107 Å³) with an increasingly greater

number of alkyl groups to encompass a different affinity for occupying 5 ($\Delta G^\circ = -(1.8-5.6)$ kcal/mol, Figure 14B). Interestingly, these spherical compounds were measured to enter 5 at rates (ΔG_{in}^\ddagger) corresponding to binding affinities ΔG° (Figure 14B): the greater the potential for occupying the basket, the faster the ingress.⁷⁹ Moreover, we found that the encapsulation kinetics/thermodynamics of I–V could be described with a quantitative relationship using the following linear equation $\Delta G_{in}^\ddagger = \rho \Delta G^\circ + \delta$ (Figure 14B). A question arose: would guest molecules, having profiles slightly different from I–V, obey the same $\Delta G^\circ/\Delta G_{in}^\ddagger$ linear free-energy relationship (LFER)? Guests VI–VII were chosen to examine this aspect of the gating (Figure 14A). 1,1,1-Trichloroethane VI is a non-spherical molecule, smaller (93 Å³) than I–V (~107 Å³). Interestingly, VI entered basket 5 at the rate faster than one would predict on the basis of the LFER in Figure 14B. Larger tetramethylsilane VII (120 Å³) was, however, found to access the basket's cavity at a rate slower than expected on the basis of the LFER in Figure 14B. Clearly, gated basket 5 selected guests on the basis of their size/shape: for isosteric guests, the encapsulation rates would track the intrinsic binding potential (ΔG°), and in accordance with the linear free-energy relationship (Figure 14B). For smaller/bigger guests, however, the rates do not fit the free-energy ($\Delta G_{in}^\ddagger = \rho \Delta G^\circ + \delta$) dependence. It follows that for two guests possessing the same affinity ΔG° for occupying a gated host, the rate by which they access its interior (ΔG_{in}^\ddagger) is a function of their size: the smaller compound is expected to enter the host at a faster while bigger molecule at a slower rate. Indeed, the quantified shape/size selectivity could be a function of the frequency by which the revolving gates flutter at the rim of 5,⁷⁸ to resemble the action of some enzymes.¹⁰⁰ On the basis of this postulate, one should find that a faster racemization of baskets contributes to a greater kinetic selectivity of trapping guests⁷⁸ yet more research is needed to test the existence of such conformational/gating selectivity³³ in artificial settings.

Stereoselective Encapsulation and Gating: As described in prior sections, three pyridine-based gates revolve at the rim of gated baskets to contribute to the formation of a racemic mixture of *P*/*M* capsules (Figure 9).⁵¹ In this vein, C₃ symmetric 5^{*P*} and 5^{*M*} possess so-called inherent chirality¹⁰¹ that is reversed by the process of racemization. By restricting the orientation of the gates to either *P* or *M* propeller-like form, however, the gated basket could perhaps become capable of kinetically discriminating (resolving) chiral molecules.¹⁰² That is to say, an enantiomeric guest (*R*) may access/depart 5^{*P*} basket should be diastereomeric and therefore comprise different stabilities! Indeed, chiral hemicarcerands⁴² and cryptophanes¹⁰³ trap/release enantiomeric guests at different rates, yet our fundamental understanding of the process and its control remain insufficient for implementing this element of design into functional hosts.¹⁰⁴

The computed structure of 5^{*P*} basket (Figure 15A)¹⁰⁵ showed that three pyridine-based gates are somewhat shifted to

the right, driving each hydrogen H_I of the CH_2 groups, away from the carbonyl oxygen atom. We, therefore, anticipated that substituting H_I with more sizeable CH_3 group (Figure 15B) should bias the helicity and give (S) - 5^P stereoisomer. In other words, by installing stereogenic S center at the "hinge" position the pyridine gates ought to assume the P orientation for

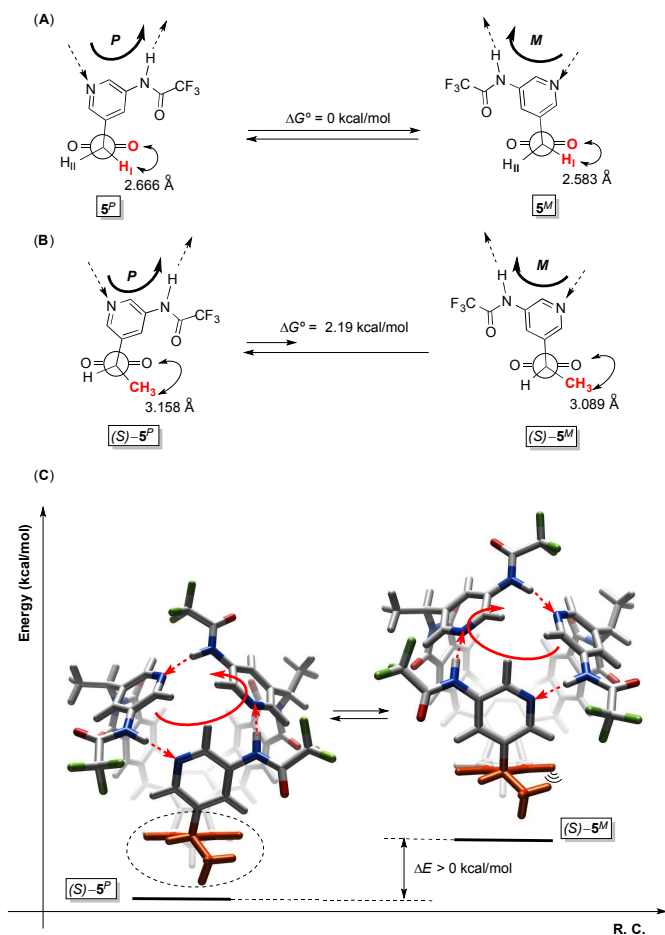


Figure 15. (A) Newman projections of P (left) and M (right) stereoisomeric forms of basket **5**. (B) Newman projections of (S) - 5^P and (S) - 5^M stereoisomeric forms. (C) Energy-minimized (DFT: RI-BP86/SV(P)) structures of diastereomeric baskets (S) - 5^P and (S) - 5^M .

minimizing the van der Waals strain.⁷⁶ Finally, we computed (DFT: RI-BP86/SV(P), Figure 15C) that (S) - 5^P is 2.19 kcal/mol more stable than the corresponding (S) - 5^M diastereomer.¹⁰⁵ The 1H NMR spectrum of (S) -**5** showed one set of signals corresponding to C_3 symmetric species, with no decoalescence of resonances at lower temperatures (up to 210 K). The results suggested a predominance of either (S) - 5^P or (R) - 5^M diastereomer. We then went on to use circular dichroism (CD) spectroscopy^{76, 77} to confirm the exclusive formation of the expected (S) - 5^P diastereomer in CD_2Cl_2 !¹⁰⁵

When enantioenriched (R) -**6** guest (>85% *ee*, Figure 16A) was added to a solution of (S) - 5^P in CD_2Cl_2 , we observed a single set of 1H NMR signals at $\delta < 0$ ppm corresponding to the haloalkane within (S) - $5^P \subset (R)$ -**6** complex (Figure 16B); likewise, the formation of (S) - $5^P \subset (S)$ -**6** ensued upon mixing (S) - 5^P and (S) -**6** (Figure 16B). Importantly, we found that

(S) - 5^P possessed an almost identical potential for complexing R -**6** ($\Delta G^\circ(R) = -0.92 \pm 0.08$ kcal/mol) and S -**6** ($\Delta G^\circ(S) = -0.86 \pm 0.06$ kcal/mol). In spite of comparable intrinsic affinities ($\Delta\Delta G^\circ(R/S) = 0.06$ kcal/mol), gated basket (S) - 5^P kinetically differentiated (1H -NMR spectroscopy)¹⁰⁵ enantiomeric 1,2-

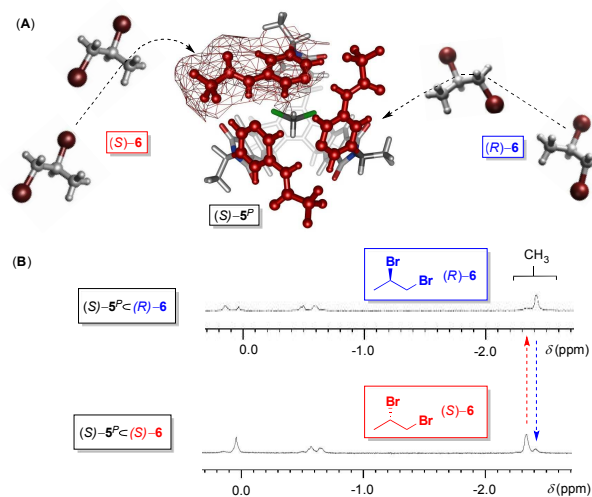


Figure 16. (A) Top view of energy-minimized structure of (S) - 5^P (RI-BP86/SV(P)) containing a molecule of CH_2Cl_2 . The unidirectional opening of this basket is suggested to permit the entrapment of enantiomeric (R) -**6** and (S) -**6**. (C) A region of 1H NMR spectrum (400 MHz, 200.0 K) of a mixture of (S) - 5^P (3.92 mM) and (R) -**6** (62.7 mM) with resonances corresponding to (S) - $5^P \subset (R)$ -**6** complex. (D) A region of 1H NMR spectrum (400 MHz, 200.0 K) of a mixture of (S) - 5^P (3.92 mM) and (S) -**6** (74.5 mM) with signals corresponding to (S) - $5^P \subset (S)$ -**6** complex.

dibromopropanes to a greater degree $\Delta\Delta G_{in}^\ddagger(R/S) = 0.3$ kcal/mol! Thus, the R -**6** guest would enter (S) - 5^P two times faster than the S -**6** compound. To explain the observation, we suggested that pyridine-based gates, residing in their principal P orientation within (S) - 5^P , unfold in a unidirectional manner during the trafficking of (R/S) -**6** (Figure 16A). In this way, the observed stereoselectivity arose from diastereomeric transition states formed in the gating.¹⁰⁵

Recently, we delineated an effective synthetic strategy for rapid preparation of C_3 symmetric **7** possessing a twisted framework and therefore a chiral inner space (Figure 17).¹⁰⁶ In particular, we used methanesulfonic acid (CH_3SO_3H) to promote a tandem of intramolecular annulation reactions (cyclialkylations)¹⁰⁷ with the conversion of indene derivative **8** into **7** (85% yield, Figure 17A). The cup-shaped **7** encompasses three [3.2.1] bicyclic rings twisted in the same direction so that the molecule is helical with either right- (P) or left-handed (M) sense of twist (Figure 17B). Twisted cavitands have unique topology¹⁰⁸ and are more sizeable than gated hosts of type **5** (Figure 5). At present, we are investigating these concave compounds for promoting stereoselective encapsulations, obtaining chiral sensors and supramolecular catalysts.^{99, 104, 109-113}

Gated Baskets and Reactivity: Self-assembled or covalent molecular capsules offer a unique environment² for destabilizing reactants and/or stabilizing reactive

intermediates/transition states of chemical reactions.^{10, 11, 13} Given the subtlety of noncovalent interactions,⁹⁷ however, it is

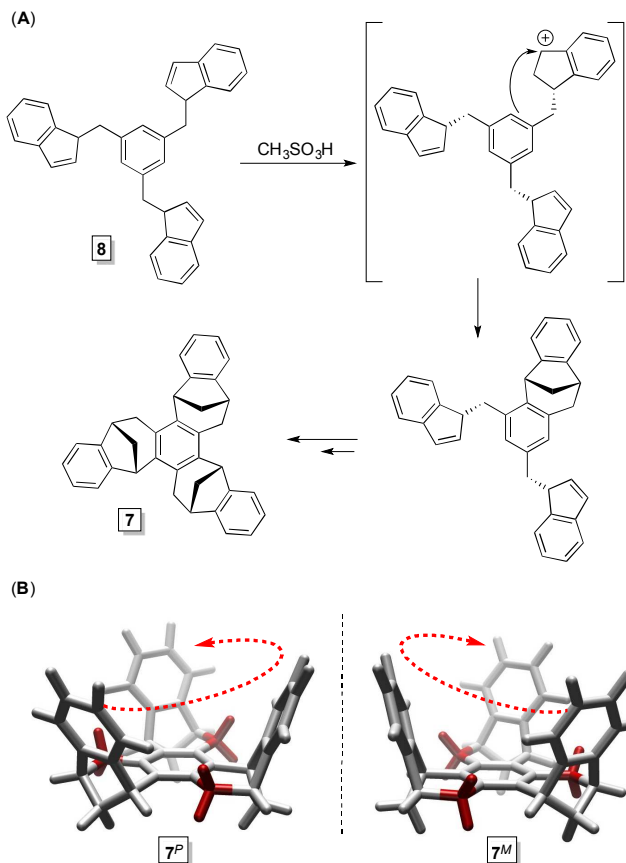


Figure 17. (A) The cyclization of **8** is promoted with $\text{CH}_3\text{SO}_3\text{H}$ to give twisted cavitand **7** (85%, $\text{CH}_2\text{ClCH}_2\text{Cl}$);¹⁰⁶ an electron-pushing scheme describes the first annulation reaction. (B) C_3 symmetric 7^P and 7^M (MMFFs, Spartan) possess a screw-shaped structure with either a right (P) or left-handed (M) sense of twist.

indeed challenging to rationally design a supramolecular (encapsulation-based) catalyst^{114, 115} whereby a combination of electrostatic forces (~ 1 kcal/mol or more) is expected to stabilize the transition state of a desired chemical transformation. In particular, the conformational changes of encapsulated guest(s) have almost uniformly been found to slow down or stay unchanged relative to those occurring in an isotropic solvent system.¹¹⁶⁻¹¹⁸ We recently reported a case of accelerated ring flipping of cyclohexane- d_{11} ($\text{C}_6\text{D}_{11}\text{H}$) within gated basket **5** (Figure 18A).⁵⁷ The rate coefficient k (s^{-1}) of cyclohexane- d_{11} undergoing chair-to-chair interconversion (Figure 18B) was, in CD_2Cl_2 ($k = 6.9 \pm 2.2 \text{ s}^{-1}$; $\Delta G^\ddagger = 10.1 \pm 0.1$ kcal/mol) and within basket **5** ($k = 43 \pm 3 \text{ s}^{-1}$; $\Delta G^\ddagger = 9.43 \pm 0.03$ kcal/mol), quantified with ^1H , ^1H -EXSY as well as dynamic NMR measurements at 189 K. As the conformational change of $\text{C}_6\text{D}_{11}\text{H}$ was roughly five times faster inside gated basket than in the reference bulk solvent, we used electronic structure methods (DFT: M06-2X, Figure 18B) to identify the origin of the observed acceleration.⁵⁷ In essence, the optimized geometry of chair cyclohexane was slightly destabilized inside the basket relative to vacuum ($\Delta E = 0.25$ kcal/mol, Figure

18B). Three $\text{C}-\text{H} \cdots \pi$ interactions ($< 2.7 \text{ \AA}$, from each hydrogen to juxtaposed π centroid, Figure 18B) were

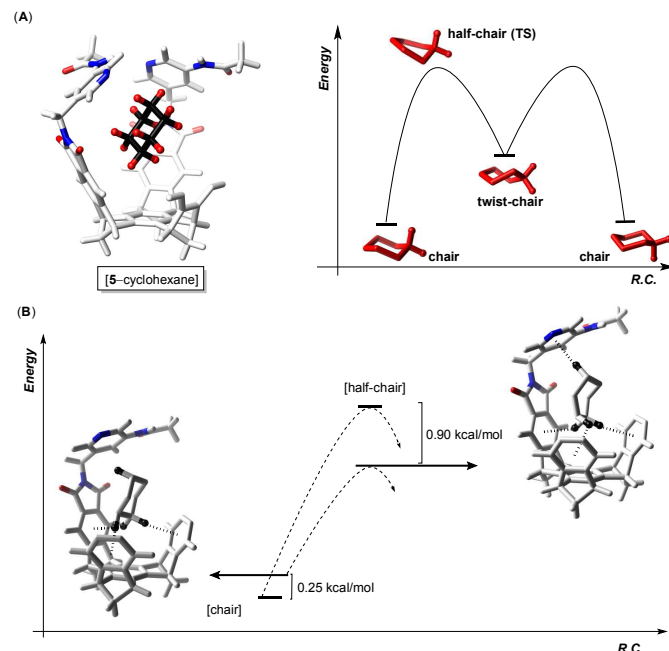


Figure 18. (A) Energy minimized structure of basket **5** containing cyclohexane (M06-2X/6-31G(d)); note that the front side of the basket is omitted for clarity. An energy diagram for the conformational interconversion of cyclohexane (right). (B) Energy optimized structures of chair (left) and half-chair (right) conformers inside gated molecular basket **5** (M06-2X/6-31G(d)); some structural features are omitted for clarity.

suggested affect the geometry of cyclohexane altering from being D_{3d} symmetric in vacuum to C_1 inside **5**. Conversely, the half-chair transition state of cyclohexane was found to be "more stable" in basket **5** than in vacuum ($\Delta E = -0.90$ kcal/mol, Figure 18B). The formation of another host-guest $\text{C}-\text{H} \cdots \pi$ interaction distorted three dihedral angles of the half-chair carbon framework moving it along the reaction coordinate to more closely resemble the twist-boat product! The activation barriers for the chair-to-chair interconversion of cyclohexane were, in this way, computed to be $\Delta E^\ddagger = 10.87$ kcal/mol in the interior of **5** while $\Delta E^\ddagger = 12.02$ kcal/mol in vacuum ($\Delta\Delta E^\ddagger = 1.15$ kcal/mol). Importantly, the result was in good agreement with our experimental measurements ($\Delta\Delta G^\ddagger = 0.5$ kcal/mol). To sum up, molecular recognition of the transition state corresponding to the interconversion of cyclohexane facilitated the transformation thereby concurring with the Pauling paradigm: "enzymes are molecules that are complementary in structure to the activated complexes of the reactions that they catalyze...".¹¹⁹

With the process of molecular gating under control, one wonders about a potential relationship between the gating of reactants and chemical reactivity. That is to say, will dynamic regulation of substrate access to a catalytic center, embedded in a gated molecular basket, have an effect on the rate of a chemical reaction taking place in the basket's interior (Figure 19A)? So far, the process of gating allows for controlling the time that molecules stay in an intimate contact.⁹⁶ By increasing

the lifetime of such an encounter complex, the reaction could become more effective on the basis of an increased probability for overcoming the activation barrier via a higher number of successful collisions (see the Menger's spatiotemporal postulate).¹²⁰ In another possible scenario, the gating could be adjusted to limit the rate of a particular chemical transformation, which could further be manipulated for controlling the outcome of a series of reactions. Since there have been no studies about gated catalysis, we set to create a family of gated catalysts.¹²¹ It, thus, occurred to us that a

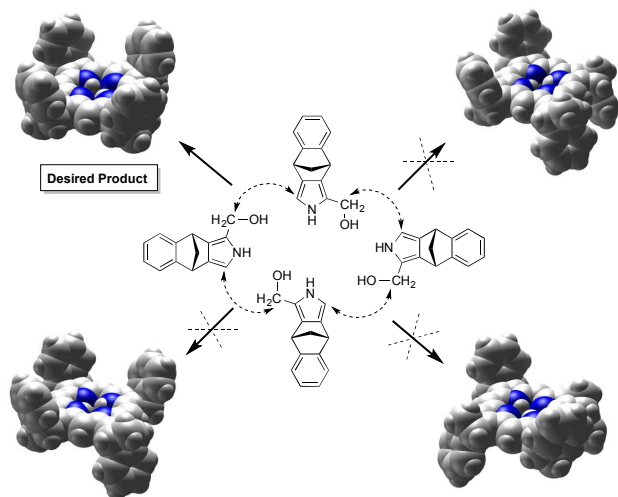


Figure 19. Energy-minimized structures (MMFFs, Spartan) of four diastereomeric porphyrins. The condensation of enantiopure pyrromethanecarbinol (but not racemate) was demonstrated to give the cup-shaped product.¹²¹

stereoselective installation of four norbornane "walls" around a porphyrin "floor" would give a basket-like host containing a porphyrin ring (Figure 19). Accordingly, we optimized a synthetic methodology for obtaining basket **9** by promoting head-to-tail tetramerization of enantiopure pyrromethanecarbinol **10** with Brønsted acids (*p*-TsOH).¹²² The reaction was under kinetic control as longer reaction times and higher concentrations of the acid led to the formation of other diastereomeric porphyrin systems (Figure 19). Importantly, basket Mn(III)-**9** (Figure 20) was expected to react with a sacrificial terminal oxidant (*t*-BuSO₂PhIO) to give an elusive Mn(V)=O species capable of transferring an oxygen atom to olefins in its spacious inner space ($V \sim 570 \text{ \AA}^3$). If the residing time of olefins is indeed controlled via gating, there should be a possibility to investigate the relationship between molecular gating and reactivity.

First, we incorporated Zn(II) into basket **9** to form Zn(II)-**9** capable of axial coordination of imidazole-based ligands. Smaller 1-methylimidazole (64 \AA^3) was found to predominantly bind to Zn(II)-**9** inside of its cavity while larger 1,5-diadamantylimidazole (361 \AA^3) would coordinate at its outer side. The rationale for these studies rested in the notion that the complexation of *N*-heterocycles to the outer side of Mn(III)-**9**

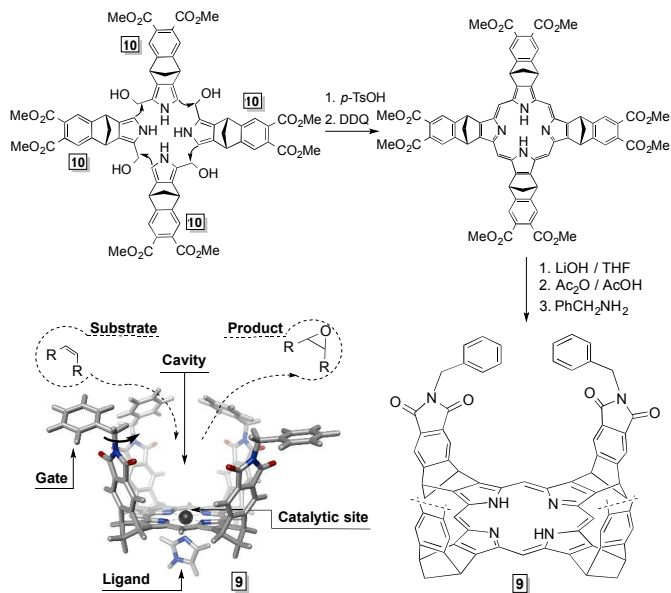


Figure 20. (A) Diastereoselective tetramerization of enantioenriched **10** (5.0 mM) was completed in CHCl₃ with *p*-TsOH (0.395 mM) at room temperature. (B) We designed molecular basket **9** (AM1, Spartan) to have a porphyrin "floor", phthalimide "walls" and aromatic "gates". The inner volume of **9**, with four gates pointing toward the cavity, was estimated to be 570 \AA^3 .

would enforce the epoxidation to occur in the cavity of the basket (Figure 21A).¹²² *N*-Heterocycles are known to bind to Mn(III) porphyrins forming five- and six-coordinate complexes. With the assistance of UV-Vis spectroscopy, we determined that Mn(III)-**9** basket would predominantly bind (a) 1-methylimidazole at its inner side ($K_{a1} = 58 \pm 13 \text{ M}^{-1}$, $K_{a2} < 5 \text{ M}^{-1}$) to give L_{in} -Mn(III)-**9** and (b) 1,5-diadamantylimidazole to the outer side ($K_{a1} = 332 \pm 26 \text{ M}^{-1}$, $K_{a2} \sim 0 \text{ M}^{-1}$) forming L_{out} -Mn(III)-**9** (Figure 21A). The epoxidation of an equimolar mixture of differently sized/shaped *cis*-2-octene **10** (187 \AA^3) and *cis*-cyclooctene **11** (142 \AA^3) was, in the presence of L_{in} -Mn(III)-**9** and L_{out} -Mn(III)-**9**, promoted with soluble iodosylarene *t*-BuSO₂PhIO in CH₂Cl₂ at room temperature (Figure 21A/B). When the reaction occurred outside the cavity of L_{in} -Mn(III)-**9**, the oxidation of the linear alkene **10** was 1.2 times faster than the cyclic one **11**. When the epoxidation reaction was taking place inside the cavity of L_{out} -Mn(III)-**9**, however, the conversion of linear alkene **10** was 2.0 times faster than the cyclic one **11**. What is the origin of the observed shape selectivity? Why would linear alkene react at a faster rate ($\Delta\Delta G^\ddagger = 0.3 \text{ kcal/mol}$) than the cyclic one in the inner space of the supramolecular catalyst? Since we could not detect the encapsulation of **10** or **11** within basket **9** (¹H NMR spectroscopy), the observed kinetic resolution could emanate from the catalyst's topology and/or its dynamic nature (gates revolving at the rim). At present, we are working on placing pyridine-based gates into **9** for forming intramolecular hydrogen-bonding contacts. The utility of such gated hosts as well as its catalytic characteristics will be evaluated.

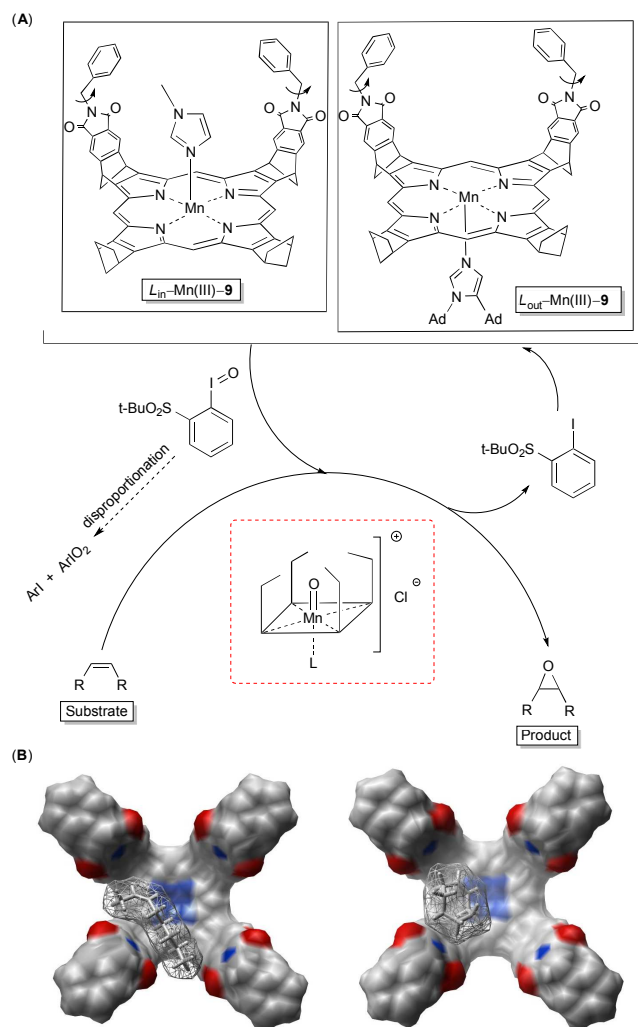


Figure 21. (A) The epoxidation of alkenes **10** and **11** was, in the presence of iodossylarene, conducted in the interior of $L_{out}\text{-Mn(III)-9}$ and at the outer face of $L_{in}\text{-Mn(III)-1}$. (B) Top view of energy-minimized (MMFF, Spartan) structures of **10** (left) and **11** (right) docked in the interior of gated basket **9** with its phenyl gates pointing away from the cavity.

Conclusions

In the last two decades, we have witnessed a growing interest toward elucidating mechanisms by which the process of molecular encapsulation takes place. At present, we recognize that conformational changes in capsular hosts could facilitate in/out trafficking of guests. Controlling the process of this so-called molecular gating¹²³ is still a matter of scientific curiosity but could become useful for modulating the outcome of chemical reactions (especially for the optimized design and operation of supramolecular catalysts) and promoting a delivery of molecules. Gated molecular baskets, described in this review, operate via unfolding their pyridine-basked gates at the rim for permitting the passage of guests. These compounds are now established as useful models for not only investigating encapsulation mechanisms but also understanding the utility of gating in controlling the outcome of chemical reactions.

Acknowledgements

This work was financially supported with funds obtained from the National Science Foundation under CHE-1305179 to J.D.B. The Ohio Supercomputer Center is gratefully acknowledged for providing generous computational resources.

Notes and references

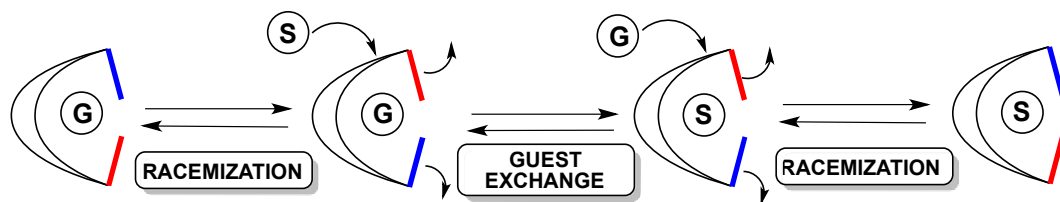
^a Department of Chemistry and Biochemistry, The Ohio State University, 100 West 18th Avenue, Columbus, OH 43210, USA. Tel: +001 614-247-8342; E-mail: badjic@chemistry.ohio-state.edu.

- U. H. Brinker, J.-L. Miesuet and Editors, *Molecular Encapsulation: Organic Reactions in Constrained Systems*, 2010.
- F. Hof, S. L. Craig, C. Nuckolls and J. Rebek, Jr., *Angew. Chem., Int. Ed.*, 2002, **41**, 1488-1508.
- D. J. Cram, J. M. Cram and Editors, *Container Molecules and Their Guests*, 1997.
- J. B. Wittenberg and L. Isaacs, *Supramol. Chem. Mol. Nanomater.*, 2012, **1**, 25-43.
- M. Rekharsky and Y. Inoue, *Supramol. Chem. Mol. Nanomater.*, 2012, **1**, 117-133.
- B. C. Gibb, *Chemosensors*, 2011, 3-18.
- K. T. Chapman and W. C. Still, *J. Am. Chem. Soc.*, 1989, **111**, 3075-3077.
- D. J. Cram, *Science*, 1983, **219**, 1177-1183.
- D. Fiedler, D. H. Leung, R. G. Bergman and K. N. Raymond, *Acc. Chem. Res.*, 2005, **38**, 349-358.
- R. J. Hooley and J. Rebek, Jr., *Chem. Biol.*, 2009, **16**, 255-264.
- M. Yoshizawa, J. K. Klosterman and M. Fujita, *Angew. Chem., Int. Ed.*, 2009, **48**, 3418-3438.
- R. Warmuth, *Eur. J. Org. Chem.*, 2001, 423-437.
- D. Fiedler, R. G. Bergman and K. N. Raymond, *Angew. Chem., Int. Ed.*, 2006, **45**, 745-748.
- T. Iwasawa, R. J. Hooley and J. Rebek, Jr., *Science*, 2007, **317**, 493-496.
- Z. Lin, J. Sun, B. Efremskova and R. Warmuth, *Chem. Eur. J.*, 2012, **18**, 12864-12872.
- S. Rieth, K. Hermann, B.-Y. Wang and J. D. Badjic, *Chem. Soc. Rev.*, 2011, **40**, 1609-1622.
- J. C. Sherman, C. B. Knobler and D. J. Cram, *J. Am. Chem. Soc.*, 1991, **113**, 2194-2204.
- J. C. Sherman and D. J. Cram, *J. Am. Chem. Soc.*, 1989, **111**, 4527-4528.
- D. J. Cram, S. Karbach, Y. H. Kim, L. Baczynskyj and G. W. Kallemeyn, *J. Am. Chem. Soc.*, 1985, **107**, 2575-2576.
- R. G. Chapman and J. C. Sherman, *J. Org. Chem.*, 1998, **63**, 4103-4110.
- J. F. Stoddart, *Chem. Soc. Rev.*, 2009, **38**, 1802-1820.
- F. M. Raymo, K. N. Houk and J. F. Stoddart, *J. Am. Chem. Soc.*, 1998, **120**, 9318-9322.
- R. Warmuth, *Supramol. Chem. Mol. Nanomater.*, 2012, **3**, 917-954.
- M. E. Tanner, C. B. Knobler and D. J. Cram, *J. Am. Chem. Soc.*, 1990, **112**, 1659-1660.
- D. J. Cram, M. E. Tanner and C. B. Knobler, *J. Am. Chem. Soc.*, 1991, **113**, 7717-7727.
- T. A. Robbins and D. J. Cram, *J. Chem. Soc., Chem. Commun.*, 1995, 1515-1516.
- M. L. C. Quan and D. J. Cram, *J. Am. Chem. Soc.*, 1991, **113**, 2754-2755.
- K. Nakamura and K. N. Houk, *J. Am. Chem. Soc.*, 1995, **117**, 1853-1854.
- K. N. Houk, K. Nakamura, C. Sheu and A. E. Keating, *Science*, 1996, **273**, 627-629.
- C. Sheu and K. N. Houk, *J. Am. Chem. Soc.*, 1996, **118**, 8056-8070.
- L. C. Palmer and J. Rebek, Jr., *Org. Biomol. Chem.*, 2004, **2**, 3051-3059.

32. F. Liu, H. Wang and K. N. Houk, *Curr. Org. Chem.*, 2013, **17**, 1470-1480.
33. H.-X. Zhou and J. A. McCammon, *Trends Biochem. Sci.*, 2010, **35**, 179-185.
34. A. Gora, J. Brezovsky and J. Damborsky, *Chem. Rev.*, 2013, **113**, 5871-5923.
35. J. Lu, E. Choi, F. Tamanoi and J. I. Zink, *Small*, 2008, **4**, 421-426.
36. A. L. Sisson, M. R. Shah, S. Bhosale and S. Matile, *Chem. Soc. Rev.*, 2006, **35**, 1269-1286.
37. S. L. Craig, S. Lin, J. Chen and J. Rebek, Jr., *J. Am. Chem. Soc.*, 2002, **124**, 8780-8781.
38. E. V. Anslyn and D. A. Dougherty, *Modern Physical Organic Chemistry*, University Science Books, 2006.
39. J. Santamaria, T. Martin, G. Hilmersson, S. L. Craig and J. Rebek, Jr., *Proc. Natl. Acad. Sci.*, 1999, **96**, 8344-8347.
40. J. Kang and J. Rebek, Jr., *Nature*, 1996, **382**, 239-241.
41. X. Wang and K. N. Houk, *Org. Lett.*, 1999, **1**, 591-594.
42. J. K. Judice and D. J. Cram, *J. Am. Chem. Soc.*, 1991, **113**, 2790-2791.
43. D. J. Cram, M. T. Blanda, K. Paek and C. B. Knobler, *J. Am. Chem. Soc.*, 1992, **114**, 7765-7773.
44. Y. Liu and R. Warmuth, *Org. Lett.*, 2007, **9**, 2883-2886.
45. V. Maslak, Z. Yan, S. Xia, J. Gallucci, C. M. Hadad and J. D. Badjic, *J. Am. Chem. Soc.*, 2006, **128**, 5887-5894.
46. Z. Yan, T. McCracken, S. Xia, V. Maslak, J. Gallucci, C. M. Hadad and J. D. Badjic, *J. Org. Chem.*, 2008, **73**, 355-363.
47. B.-Y. Wang, X. Bao, S. Stojanovic, C. M. Hadad and J. D. Badjic, *Org. Lett.*, 2008, **10**, 5361-5364.
48. F. Fabris, C. Zonta, G. Borsato and O. De Lucchi, *Acc. Chem. Res.*, 2011, **44**, 416-423.
49. B.-Y. Wang, X. Bao, Z. Yan, V. Maslak, C. M. Hadad and J. D. Badjic, *J. Am. Chem. Soc.*, 2008, **130**, 15127-15133.
50. J. L. Cook, C. A. Hunter, C. M. R. Low, A. Perez-Velasco and J. G. Vinter, *Angew. Chem., Int. Ed.*, 2008, **47**, 6275-6277.
51. Y. Ruan, B.-Y. Wang, J. M. Erb, S. Chen, C. M. Hadad and J. D. Badjic, *Org. Biomol. Chem.*, 2013, **11**, 7667-7675.
52. N. R. Voss and M. Gerstein, *Nucleic Acids Res.*, 2010, **38**, W555-W562.
53. M. Kamieth, F.-G. Klarner and F. Diederich, *Angew. Chem., Int. Ed.*, 1998, **37**, 3303-3306.
54. A. Collet, *Compr. Supramol. Chem.*, 1996, **2**, 325-365.
55. S. Mecozzi and J. Rebek, Jr., *Chem.-Eur. J.*, 1998, **4**, 1016-1022.
56. K. Hermann, S. Rieth, H. A. Taha, B.-Y. Wang, C. M. Hadad and J. D. Badjic, *Beilstein J. Org. Chem.*, 2012, **8**, 90-99, No 99.
57. L. Xiaoayong, W. Bao-Yu and J. D. Badjic, *Submitted for publication*, 2014.
58. B. M. Neilson and C. W. Bielawski, *J. Am. Chem. Soc.*, 2012, **134**, 12693-12699.
59. R. S. Stoll, M. V. Peters, A. Kuhn, S. Heiles, R. Goddard, M. Buhl, C. M. Thiele and S. Hecht, *J. Am. Chem. Soc.*, 2009, **131**, 357-367.
60. D. Sud, T. B. Norsten and N. R. Branda, *Angew. Chem., Int. Ed.*, 2005, **44**, 2019-2021.
61. B. L. Feringa, W. R. Browne, *Molecular Switches: Second, Completely Revised and Enlarged Edition, Volume 1*, 2011.
62. B. L. Feringa, *AIP Conf. Proc.*, 2013, **1519**, 73-75.
63. W. R. Browne, D. Pijper, M. M. Pollard and B. L. Feringa, *Chirality Nanoscale*, 2009, 349-390.
64. N. N. P. Moonen, A. H. Flood, J. M. Fernandez and J. F. Stoddart, *Top. Curr. Chem.*, 2005, **262**, 99-132.
65. H. Xu, S. P. Stamp and D. M. Rudkevich, *Org. Lett.*, 2003, **5**, 4583-4586.
66. S. Shinkai, T. Ogawa, T. Nakaji, Y. Kusano and O. Nanabe, *Tetrahedron Lett.*, 1979, **19**, 4569-4572.
67. T. Gottschalk, B. Jaun and F. Diederich, *Angew. Chem., Int. Ed.*, 2007, **46**, 260-264.
68. P. Amrhein, A. Shivanyuk, D. W. Johnson and J. Rebek, Jr., *J. Am. Chem. Soc.*, 2002, **124**, 10349-10358.
69. H. Abe, N. Masuda, M. Waki and M. Inouye, *J. Am. Chem. Soc.*, 2005, **127**, 16189-16196.
70. B. Zheng, F. Wang, S. Dong and F. Huang, *Chem. Soc. Rev.*, 2012, **41**, 1621-1636.
71. X. Yan, F. Wang, B. Zheng and F. Huang, *Chem. Soc. Rev.*, 2012, **41**, 6042-6065.
72. G. Yu, M. Xue, Z. Zhang, J. Li, C. Han and F. Huang, *J. Am. Chem. Soc.*, 2012, **134**, 13248-13251.
73. G. Yu, X. Zhou, Z. Zhang, C. Han, Z. Mao, C. Gao and F. Huang, *J. Am. Chem. Soc.*, 2012, **134**, 19489-19497.
74. S. Rieth, B.-Y. Wang, X. Bao and J. D. Badjic, *Org. Lett.*, 2009, **11**, 2495-2498.
75. S. Rieth, Z. Yan, S. Xia, M. Gardlik, A. Chow, G. Fraenkel, C. M. Hadad and J. D. Badjic, *J. Org. Chem.*, 2008, **73**, 5100-5109.
76. S. Stojanovic, D. A. Turner, C. M. Hadad and J. D. Badjic, *Chem. Sci.*, 2011, **2**, 752-759.
77. S. Stojanovic, D. A. Turner, A. I. Share, A. H. Flood, C. M. Hadad and J. D. Badjic, *Chem. Commun.*, 2012, **48**, 4429-4431.
78. S. Rieth and J. D. Badjic, *Chem. Eur. J.*, 2011, **17**, 2562-2565.
79. S. Rieth, X. Bao, B.-Y. Wang, C. M. Hadad and J. D. Badjic, *J. Am. Chem. Soc.*, 2010, **132**, 773-776.
80. J. J. Led, H. Gesmar and F. Abildgaard, *Methods Enzymol.*, 1989, **176**, 311-329.
81. C. L. Perrin and T. J. Dwyer, *Chem. Rev.*, 1990, **90**, 935-967.
82. I. Vatsouro, E. Alt, M. Vysotsky and V. Boehmer, *Org. Biomol. Chem.*, 2008, **6**, 998-1003.
83. I. Vatsouro, V. Rudzevich and V. Boehmer, *Org. Lett.*, 2007, **9**, 1375-1377.
84. M. O. Vysotsky and V. Boehmer, *Org. Lett.*, 2000, **2**, 3571-3574.
85. M. O. Vysotsky, I. Thondorf and V. Boehmer, *Chem. Commun.*, 2001, 1890-1891.
86. R. J. Hooley, H. J. Van Anda and J. Rebek, Jr., *J. Am. Chem. Soc.*, 2006, **128**, 3894-3895.
87. A. V. Davis, R. M. Yeh and K. N. Raymond, *Proc. Natl. Acad. Sci.*, 2002, **99**, 4793-4796.
88. S. Liu, H. Gan, A. T. Hermann, S. W. Rick and B. C. Gibb, *Nat. Chem.*, 2010, **2**, 847-852.
89. T. V. Nguyen, H. Yoshida and M. S. Sherburn, *Chem. Commun.*, 2010, **46**, 5921-5923.
90. R. C. Helgeson, A. E. Hayden and K. N. Houk, *J. Org. Chem.*, 2010, **75**, 570-575.
91. K. Otsuka, T. Kondo, R. Nishiyabu and Y. Kubo, *J. Org. Chem.*, 2013, **78**, 5782-5787.
92. Z. Yan, Y. Chang, D. Mayo, V. Maslak, S. Xia and J. D. Badjic, *Org. Lett.*, 2006, **8**, 3697-3700.
93. J. K. M. Sanders, *Chem. Eur. J.*, 1998, **4**, 1378-1383.
94. P. Thordarson, E. J. A. Bijsterveld, A. E. Rowan and R. J. M. Nolte, *Nature*, 2003, **424**, 915-918.
95. J. Wang and B. L. Feringa, *Science*, 2011, **331**, 1429-1432.
96. B.-Y. Wang, S. Rieth and J. D. Badjic, *J. Am. Chem. Soc.*, 2009, **131**, 7250-7252.
97. C. A. Hunter, *Angew. Chem., Int. Ed.*, 2004, **43**, 5310-5324.
98. K. C. Harper, E. N. Bess and M. S. Sigman, *Nat. Chem.*, 2012, **4**, 366-374.
99. Y. Ruan, E. Dalkilic, P. W. Peterson, A. Pandit, A. Dastan, J. D. Brown, S. M. Polen, C. M. Hadad and J. D. Badjic, *Chem. Eur. J.*, 2014, **20**, 4251-4256.
100. H.-X. Zhou, S. T. Wlodek and J. A. McCammon, *Proc. Natl. Acad. Sci.*, 1998, **95**, 9280-9283.
101. A. Szumna, *Chem. Soc. Rev.*, 2010, **39**, 4274-4285.
102. M. A. Mateos-Timoneda, M. Crego-Calama and D. N. Reinhoudt, *Chem. Soc. Rev.*, 2004, **33**, 363-372.
103. C. Givelet, J. Sun, D. Xu, T. J. Emge, A. Dhokte and R. Warmuth, *Chem. Commun.*, 2011, **47**, 4511-4513.
104. J. Meeuwissen and J. N. H. Reek, *Nat. Chem.*, 2010, **2**, 615-621.
105. B.-Y. Wang, S. Stojanovic, D. A. Turner, T. L. Young, C. M. Hadad and J. D. Badjic, *Chem. Eur. J.*, 2013, **19**, 4767-4775.
106. K. Hermann, D. A. Turner, C. M. Hadad and J. D. Badjic, *Chem. Eur. J.*, 2012, **18**, 8301-8305.
107. Y. Koltunov Konstantin, G. K. S. Prakash, G. Rasul and A. Olah George, *J. Org. Chem.*, 2002, **67**, 4330-4336.
108. J. D. Badjic, S. Stojanovic and Y. Ruan, *Adv. Phys. Org. Chem.*, 2011, **45**, 1-34.
109. C. Moberg, *Angew. Chem., Int. Ed.*, 2006, **45**, 4721-4723.
110. S. E. Gibson and M. P. Castaldi, *Chem. Commun.*, 2006, 3045-3062.

111. L. A. Joyce, M. S. Maynor, J. M. Dregna, G. M. da Cruz, V. M. Lynch, J. W. Canary and E. V. Anslyn, *J. Am. Chem. Soc.*, 2011, **133**, 13746-13752.
112. S. Chen, Y. Ruan, J. D. Brown, J. Gallucci, V. Maslak, C. M. Hadad and J. D. Badjic, *J. Am. Chem. Soc.*, 2013, **135**, 14964-14967.
113. Y. Ruan, H. A. Taha, R. J. Yoder, V. Maslak, C. M. Hadad and J. D. Badjic, *J. Phys. Chem. B*, 2013, **117**, 3240-3249.
114. M. Raynal, P. Ballester, A. Vidal-Ferran and P. W. N. M. van Leeuwen, *Chem. Soc. Rev.*, 2014, **43**, 1734-1787.
115. M. Raynal, P. Ballester, A. Vidal-Ferran and P. W. N. M. van Leeuwen, *Chem. Soc. Rev.*, 2014, **43**, 1660-1733.
116. M. D. Pluth, R. G. Bergman and K. N. Raymond, *J. Org. Chem.*, 2008, **73**, 7132-7136.
117. T. Gottschalk, P. D. Jarowski and F. Diederich, *Tetrahedron*, 2008, **64**, 8307-8317.
118. B. M. O'Leary, R. M. Grotzfeld and J. Rebek, Jr., *J. Am. Chem. Soc.*, 1997, **119**, 11701-11702.
119. X. Zhang and K. N. Houk, *Acc. Chem. Res.*, 2005, **38**, 379-385.
120. F. M. Menger, *Acc. Chem. Res.*, 1985, **18**, 128-134.
121. B.-Y. Wang, D. A. Turner, T. Zujovic, C. M. Hadad and J. D. Badjic, *Chem. Eur. J.*, 2011, **17**, 8870-8881, S8870/8871-S8870/8851.
122. B.-Y. Wang, T. Zujovic, D. A. Turner, C. M. Hadad and J. D. Badjic, *J. Org. Chem.*, 2012, **77**, 2675-2688.
123. F. Liu, R. C. Helgeson and K. N. Houk, *Acc. Chem. Res.*, 2014, in press.

Table of Contents



The process of molecular gating is important for controlling the trafficking of guests to and from artificial molecular capsules.

Biography



Keith Hermann received his B.S. in Chemistry from Northern Illinois University while working towards the total synthesis of Riccardin C analogs. He is currently a senior graduate student at the Ohio State University, having spent his graduate career designing, developing the synthesis and probing the encapsulation characteristics of molecular baskets. His other research interests include non-covalent surface modifications and their application in molecular electronics.



Yian Ruan received her B.S. in chemistry and biology from Tsinghua University in China (2008). She obtained her PhD degree in organic chemistry from the Ohio State University (2014) by designing, preparing and investigating the characteristics of molecular baskets capable of trapping nerve agents. Her research interests include molecular encapsulation and self-assembled materials.



Jovica D. Badjic is a Professor of Chemistry at the Ohio State University. He received his diploma in chemistry from the University of Belgrade (1994) and Ph.D. in organic chemistry from Iowa State University (2001). He was a postdoctoral fellow in the group of J. Fraser Stoddart (UCLA) studying multivalency and its utility in artificial systems. His research interest is in the area of molecular encapsulation and particularly centered on understanding the role of encapsulation in supramolecular catalysis and the preparation of dynamic nanostructured materials.



Christopher M. Hadad is a Professor of Chemistry and Biochemistry at the Ohio State University. He received his B.S. degree in chemistry from the University of Delaware (1987) and Ph.D. in organic chemistry from Yale University (1993), working with Professor Kenneth B. Wiberg. He was an NSF postdoctoral fellow in the research group of Professor Charles H. DePuy (University of Colorado). His research interests are focused in the areas of organic and biological reactive intermediates, specifically for their roles in energy applications, photoaffinity labeling, photochemistry, reactive oxygen species, combustion, atmospheric chemistry, and for developing therapeutics against exposure to organophosphorus chemical nerve agents.



Alex M. Hardin graduated from Missouri State University in 2010 with a B.S. in Chemistry, studying solid-state NMR of oligonucleotides. Currently a graduate student in the research group of Professor Jovica D. Badjic at the Ohio State University, he is interested in supramolecular architecture, host-guest chemistry, and organic semiconductors.